Biochemical and Biophysical Research Communications 425 (2012) 256–260

Contents lists available at SciVerse ScienceDirect

Biochemical and Biophysical Research Communications

journal homepage: www.elsevier.com/locate/ybbrc

Small-angle X-ray scattering reveals structural dynamics of the botulinum neurotoxin associating protein, nontoxic nonhemagglutinin

Yoshimasa Sagane [a,1], Shin-Ichiro Miyashita [a,1], Keita Miyata [a,b,1], Takashi Matsumoto [c], Ken Inui [a,b], Shintaro Hayashi [a], Tomonori Suzuki [d], Kimiko Hasegawa [c], Shunsuke Yajima [e], Akihito Yamano [c], Koichi Niwa [a], Toshihiro Watanabe [a,*]

[a] Department of Food and Cosmetic Science, Faculty of Bioindustry, Tokyo University of Agriculture, 196 Yasaka, Abashiri 099-2493, Japan
[b] Japan Society for the Promotion of Science, 1-8 Chiyoda-ku, Tokyo 102-8472, Japan
[c] Rigaku Corporation, 3-9-12 Matsubara-Cho, Akishima 196-8666, Japan
[d] Department of Bacteriology, Okayama University Graduate School of Medicine, Dentistry and Pharmaceutical Sciences, 2-5-1 Shikata-cho, Kita-ku, Okayama 700-8558, Japan
[e] Department of Bioscience, Tokyo University of Agriculture, Faculty of Applied Bioscience, Setagaya-ku, Tokyo 156-8502, Japan

ARTICLE INFO

Article history:
Received 8 July 2012
Available online 22 July 2012

Keywords:
Clostridium botulinum
Botulinum neurotoxin
Nontoxic nonhemagglutinin
X-ray crystallographic analysis
Small-angle X-ray scattering
Structural dynamics

ABSTRACT

In cell culture supernatants, the botulinum neurotoxin (BoNT) exists as part of a toxin complex (TC) in which nontoxic nonhemagglutinin (NTNHA) and/or hemagglutinins (HAs) are assembled onto the BoNT. A series of investigations indicated that formation of the TC is vital for delivery of the toxin to nerve cells through the digestive tract. In the assembly process, BoNT binds to NTNHA yielding M-TC, and it then matures into L-TC by further association with the HAs via NTNHA in the M-TC. Here, we report a crystal structure of the NTNHA from *Clostridium botulinum* serotype D strain 4947. Additionally, we performed small-angle X-ray scattering (SAXS) analysis of the NTNHA and the M-TC to elucidate the solution structure. The crystal structure of D-4947 NTNHA revealed that BoNT and NTNHA share a closely related structure consisting of three domains. The SAXS image indicated that, even though the N-terminal two-thirds of the NTNHA molecule had an apparently similar conformation in both the crystal and solution structures, the C-terminal third of the molecule showed a more extended structure in the SAXS image than that seen in the crystallographic image. The discrepancy between the crystal and solution structures implies a high flexibility of the C-terminal third domain of NTNHA, which is involved in binding to BoNT. Structural dynamics of the NTNHA molecule revealed by SAXS may explain its binding to BoNT to form the BoNT/NTNHA complex.

© 2012 Elsevier Inc. All rights reserved.

1. Introduction

Botulinum neurotoxin (BoNT; 150 kDa), produced in seven distinct serotypes (A–G) by an anaerobic gram-positive bacterium *Clostridium botulinum*, is the most potent toxin in nature. BoNT enters humans and animals via one of three pathways: toxin production by colonized bacterium in the gastrointestinal tract of the infant, entrance of the toxin through a wound, and oral ingestion of the toxin with polluted foods. Among these, the latter pathway, namely food-borne botulism, is the most frequent. In any case, BoNT eventually enters neuronal cells at neuromuscular junctions, where it cleaves a specific protein involved in neurotransmitter release, causing paralysis of the muscle.

Pure BoNT is highly susceptible to proteolysis, and it easily degrades into inactive small fragments in the digestive environment [1]. Thus pure BoNT exhibits only weak or no oral toxicity. BoNT can tolerate proteolytic attack by forming a toxin complex (TC) in which it is conjugated with a 130-kDa nontoxic nonhemagglutinin (NTNHA) and/or three types of hemagglutinins (HAs) with molecular masses of 70, 33 and 17 kDa (HA-70, HA-33 and HA-17, respectively). In particular, the association of BoNT with NTNHA yields an amazingly stable complex against acidic and proteolytic conditions, while free-form BoNT is degraded into small fragments within a few hours in the presence of pepsin [1]. Additionally, the HAs, especially HA-33, facilitate its transport efficiency across intestinal epithelial and aortic endothelial cell layers [2,3].

Some studies have indicated that the TC is constructed from its constituent molecules in an orderly manner [4–6]. Association of a single BoNT and a single NTNHA forms a 280-kDa M-TC. Three HA-70 molecules bind to M-TC via NTNHA yielding the 490-kDa M-TC/HA-70. Finally, further conjugation of the three HA-33/HA-17 complexes (single HA-17 molecule plus two HA-33 molecules) onto the M-TC/HA-70 through binding of HA-17 to HA-70 leads to a mature

* Corresponding author. Fax: +81 152 48 2940.
E-mail address: t-watana@bioindustry.nodai.ac.jp (T. Watanabe).
[1] These authors contributed equally to this work.

0006-291X/$ - see front matter © 2012 Elsevier Inc. All rights reserved.
http://dx.doi.org/10.1016/j.bbrc.2012.07.077

750-kDa L-TC represented by a 14-mer model. The NTNHA molecule plays an important role in the assembly pathway that connects BoNT and HAs. Very recently, the X-ray crystallographic structure of serotype A M-TC was reported [7]. This structure indicated that the NTNHA protein possesses a structure that is quite similar to BoNT, and that could be divided into three domains similar to BoNT. These domains were designated by reference to those of BoNT, namely nLc, nHcN, and nHcC corresponding to the light chain (Lc), the N-terminal heavy chain (HcN) and the C-terminal heavy chain (HcC), respectively. The crystal structure of M-TC indicated that NTNHA and BoNT form a compact interlocked complex.

In the current study, we describe the crystal and solution structures of NTNHA from *C. botulinum* serotype D strain 4947 (D-4947) by X-ray crystallographic and small-angle X-ray scattering (SAXS) analyses, respectively. The data obtained here indicate a discrepancy between the crystal and solution structures of the C-terminal part of the NTNHA molecule. This discrepancy may explain the interlocking of BoNT and NTNHA to form a stable M-TC structure.

2. Materials and methods

2.1. Production and purification of M-TC and recombinant NTNHA

Production and purification of D-4947 M-TC was performed using a method reported previously [8,9]. TC species were purified from culture supernatants by three consecutive chromatographic runs, on a TOYOPEARL SP-650S (Tosoh, Tokyo, Japan) cation-exchange column, a HiLoad 16/60 Superdex 200 pg (GE Healthcare, Little Chalfont, UK) gel-filtration column and a Mono S HR 5/5 (GE Healthcare) cation-exchange column. The fractions containing M-TC, identified by SDS- and native-PAGE banding profiles, were collected.

Production and purification of the recombinant NTNHA (rNTNHA; D-4947) were performed using a method reported previously [1]. *Escherichia coli* BL21 cells harboring a pET200/D-TOPO-*ntnha* vector, in which the NTNHA gene is ligated downstream of the 6x His-tag coding sequence, were cultured in 20 ml of LB broth containing 100 μg/ml kanamycin at 37 °C overnight with mild shaking. The culture was inoculated into 800 ml of fresh LB broth and cultured at 37 °C until the culture reached mid-log-phase. The production of rNTNHA was induced by IPTG (0.1 mM). After 18 h incubation at 18 °C, cells in the culture were collected and suspended in 80 ml of 50 mM phosphate buffer (pH 7.4) containing 0.3 M NaCl. The cell suspension was sonicated and centrifuged at 10,000*g* for 20 min at 4 °C. The supernatant was suspended with 5 ml of 50% Ni-Charged Resin suspension (Bio-Rad, Hercules, CA) equilibrated with 50 mM phosphate buffer (pH 7.4) containing 0.3 M NaCl. The resin mixture was poured into a glass column and rinsed with the same buffer. The bound protein was eluted with equilibration buffer containing 300 mM imidazole. The eluted fraction containing rNTNHA was precipitated with ammonium sulfate at 80% saturation. The pellets were dissolved and dialyzed against 50 mM phosphate buffer (pH 6.0) containing 0.15 M NaCl and then applied to a Superdex 200 HR 10/30 (GE Healthcare) gel-filtration column equilibrated with the same buffer. The purity of the eluted proteins was judged by SDS–PAGE.

2.2. Structural determination and crystallographic refinement of rNTNHA

X-ray diffraction data of the rNTNHA crystal [10] was integrated and scaled using the CrystalClear package (Rigaku, Tokyo, Japan). Subsequent data manipulation was carried out using the CCP4 program package [11]. An initial phase set was calculated by molecular replacement using MOLREP [12]. The search model for molecular replacement was the structure of NTNHA in M-TC from serotype A (PDB code 3V0B), which showed a high sequence identity (65.9%) to D-4947 NTNHA.

Model building was performed using the program Coot [13], and model refinement was conducted using the program Refmac5 [14]. Coordinates have been deposited to the Protein Data Bank with the accession code: 3VUO. Details of data collection and refinement are summarized in Table 1. Figures were prepared with the program CCP4 mg [15] and PyMOL (DeLano Scientific).

Table 1
Summary of data collection and refinement statistics for D-4947 NTNHA (PDB code 3VUO).

Data set name	NTNHA
X-ray diffraction data	
Wavelength (Å)	1.5418
Space group	$P3_221$
Unit cell (Å)	a = 147.85 b = 147.85 c = 229.74
Observations	79904
Unique reflections	25867
Resolutions (Å)	31.08–3.90 (4.04–3.90)
Completeness (%)	95.7 (95.7)
I/σ (I)	4.5 (2.3)
R_{merge} (%)[a]	17.4 (35.6)
Refinement statistics	
Resolution (Å)	20.00–3.90
R-factor (%)	30.10
R-free (%)	35.80
Bond length (Å)	0.011
Bond angle (°)	1.752
Ramachandran plot (%)	
Favored region	87.8
Additionally allowed region	8.7

The numbers in parentheses are given for the highest resolution shells.
[a] $R_{merge} = \sum_h\sum_j|I_{hj} - <I_h>|/\sum_h\sum_j|I_{hj}|$, where h represents a unique reflection and j represents symmetry-equivalent indices. I is the observed intensity and $\langle I\rangle$ is the mean value of I.

2.3. Small-angle X-ray scattering analysis

Small-angle X-ray scattering (SAXS) measurements of the M-TC (5 mg/ml) and the rNTNHA (1 mg/ml) in 50 mM acetate buffer (pH 5.0) were carried out on a Rigaku BioSAXS-1000 using 10–20 μl of protein solution. A total of eight datasets were collected after 120 min exposure (15 min per data set). Raw data were analyzed using the SAXSLab software package (Rigaku). SAXS curves were generated after subtracting the scattering due to the solvent in the protein solution, using the program PRIMUS [16] from the ATSAS package [17].

3. Results and Discussion

3.1. X-ray crystallography of the rNTNHA

Crystals of the rNTNHA protein were obtained using the hanging-drop vapor diffusion method as described previously [10]. Diffraction data obtained in the report was employed for the determination of X-ray crystal structure of the rNTNHA at 3.9-angstrom resolution by molecular replacement using the NTNHA structure in serotype A M-TC [7]. The final model (Fig. 1) was refined to an R-factor of 30.10% and a free R-factor of 35.80%. The three-dimensional structure of rNTNHA can be divided into three domains named nLc, nHcN and nHcC, similar to serotype A NTNHA, as well as all serotypes of the BoNT protein, as reported previously [7]. Very recently, we demonstrated that these three domains are closely related to zinc-dependent metalloproteinase-like, BoNT coiled-coil motif and concanavalin A-like domains in the SCOP database, respectively [18].

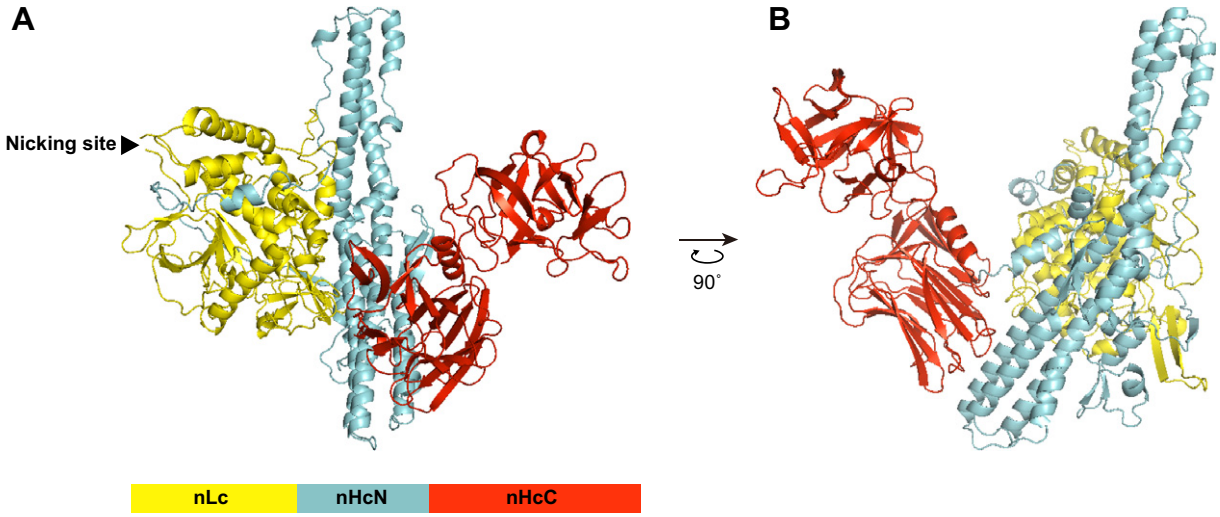

Fig. 1. Crystal structure of the recombinant NTNHA from D-4947. Three domains, *e.g.* nLc in yellow, nHcN in light blue and nHcC in red, were designated based on the domain name of BoNT. (A) Crystal structure of the D-4947 NTNHA represented by a ribbon diagram. The nicking site due to spontaneous cleavage during long-term incubation is indicated by an arrowhead. (B) Ribbon diagram of the NTNHA crystal structure that is rotated 90° clockwise around the y-axis. (For interpretation of the references to color in this figure legend, the reader is referred to the web version of this article.)

The model includes 1151 amino acid residues, whereas the whole NTNHA molecule consists of 1196 amino acid residues. Missing residues are Gly114–Gly148, Tyr442–Asp448, Pro1127 and Asp1181–Asn1182. These residues are all located in solvent-exposed regions. The X-ray crystal structure of the serotype A NTNHA, which is employed as a template for homology modeling, contains two missing regions. These regions correspond to the former two missing regions (Gly114–Gly148 and Tyr442–Asp448) in D-4947 NTNHA. In earlier studies, the NTNHA molecules produced by native *C. botulinum* strain D-4947 [9] and transformed *E. coli* [1] were found to be spontaneously converted to the nicked form via excision of several residues at a specific site. The missing region, Gly114–Gly148, was consistent with the excised region in the nicked form of NTNHA. The missing residues Tyr442–Asp448 in D-4947 NTNHA, and the corresponding region in a serotype A molecule, would be too flexible in the crystal to be detected by X-ray analysis. The remaining two short missing regions (Pro1127 and Asp1181–Asn1182) in D-4947 NTNHA might have occurred due to gaps in the sequence alignment.

The NTNHA molecule shares a similar β-trefoil folding at its C-terminal (nHcC domain) with the BoNT, HA-33 and HA-17 molecules. β-trefoil folding is often found in proteins that function in recognition and binding to oligosaccharides, *e.g.* lectins such as the ricin B chain and *Amaranthus caudatus* agglutinin, and cytokines such as interleukin-1 and fibroblast growth factor [19]. In a previous study, we demonstrated that cell binding and transport across the cell monolayer in the rat intestinal epithelial cell of botulinum M-TC (BoNT/NTNHA) and L-TC (M-TC/HAs) arose via BoNT and HA-33, respectively, in a sialic acid-dependent manner [20]. The NTNHA molecule may also possess an oligosaccharide recognition ability that should be addressed in the near future. Additionally, the nHcC domain displayed considerably lower electron density.

3.2. Structural dynamics of NTNHA revealed by SAXS image

The rNTNHA was subjected to SAXS analysis to determine its solution structure. The radius of gyration (R_g) and maximum particle dimension (D_{max}) of the rNTNHA were calculated from SAXS to be 55.52 and 220 angstroms, respectively. The rNTNHA crystallographic structure was docked into the SAXS dummy residue model (DRM) manually. The SAXS-derived DRM of the rNTNHA with the best-fitted crystallographic structure is shown in Fig. 2A and Supplementary video 1. The docking image indicated that SAXS DRM could be fitted to the nLc and nHcN domains in the crystallographic structure. On the other hand, in this docking image, the nHcC domain in the crystallographic structure could not be superposed onto the SAXS DRM. Additionally, we performed SAXS analysis on the D-4947 M-TC (BoNT/NTNHA complex). The R_g and D_{max} of the M-TC were estimated from the SAXS to be 46.76 and 150, respectively. These values were lower than those of the NTNHA protein, even though the total molecular mass of M-TC is twice that of NTNHA. SAXS DRM of rNTNHA was docked into that of the M-TC manually, and the best-fitted image is shown in Fig. 2B and Supplementary video 2. The image clearly demonstrates that the extended structure of the rNTNHA model, which resembled a "tail", could not be included in the M-TC SAXS DRM envelope.

Based on the crystal structure, the inter-domain angles made by axes of the HcN and HcC domains were significantly different (~120°) between serotype A/B and E BoNTs [21], suggesting that the linker between the two BoNT domains allows flexibility. Since BoNT and NTNHA share similar three-dimensional structures and secondary structure organizations, the linker between nHcN and nHcC should also be flexible. Supplementary video 3 (summarized in Fig. 3) shows a working model of the flexible NTNHA structure based on a comparison between the crystallographic and SAXS images. The nLc and nHcN displayed very similar appearances in both the crystallographic and the SAXS images, and thus these domains would be stationary in solution. On the other hand, the remaining area in the SAXS image does not fit to the nHcC domain in the crystallographic image. A "wing" like mobility model of the nHcC domain would explain this discrepancy. That is, the nHcC domain can iteratively move from an orthogonal orientation against the stationary domain, which corresponds to the crystallographic image, to a straight, laterally directed orientation. SAXS images obtained in this study may represent a merged aspect of the nHcC domain swinging around the linker between nHcN and nHcC. However, this model does not include the "tail" like extended structure observed in the SAXS image. The nHcC domain displayed low electron density in the crystallographic image, suggesting flexibility of this domain. The "tail" like aspect in the SAXS image may imply an extension of the nHcC domain when it got into a straight

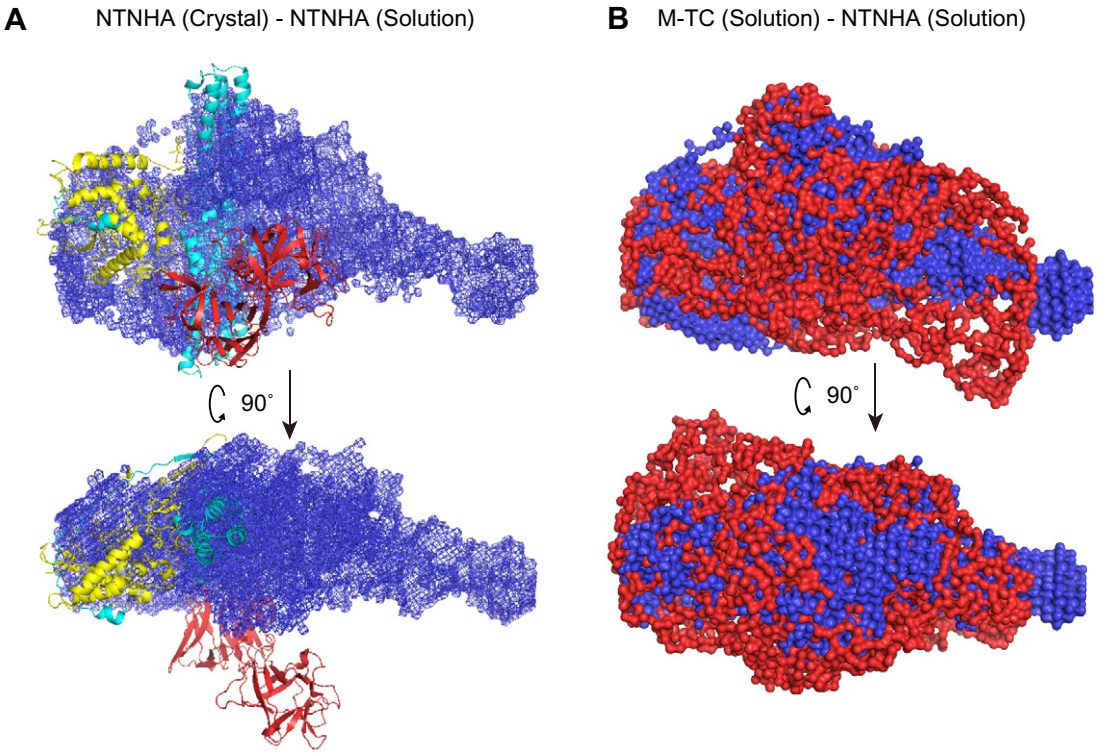

Fig. 2. Crystal and solution structure of the NTNHA. (A) The crystal structure image indicated by a three-domain model with nLc in yellow, nHcN in light blue and nHcC in red is superimposed onto the solution structure image (blue) determined by SAXS. The superposed image implies that the nLc and nHcN display a similar form in both the crystal and solution structure, whereas the nHcC shows a discrepancy between the crystal and solution structures. (B) Solution structure of M-TC and NTNHA. SAXS image of the NTNHA (blue) is superposed onto that of the M-TC (red). (For interpretation of the references to color in this figure legend, the reader is referred to the web version of this article.)

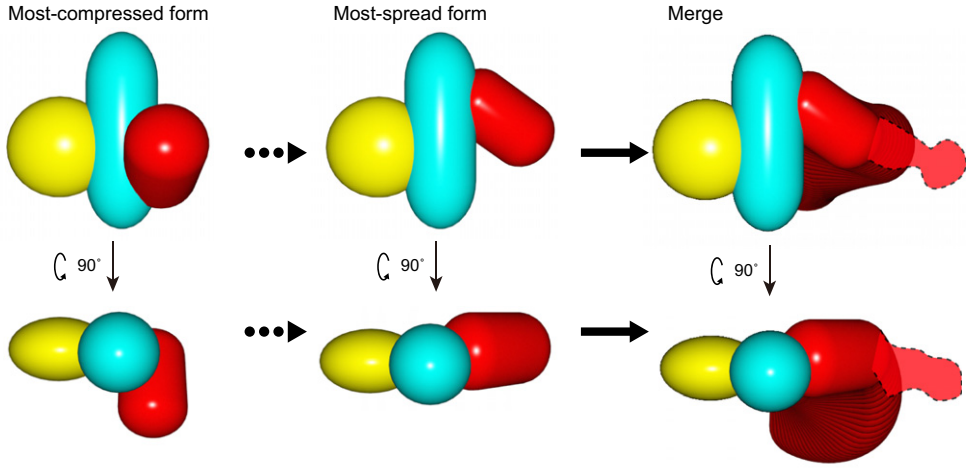

Fig. 3. Hypothetical "wing" model for the NTNHA molecule. The nLc, nHcN and nHcC are represented by yellow, light blue and red ellipses, respectively. "Most-compressed form" NTNHA model (left) is illustrated based on the crystal structure of NTNHA. In the solution structure, the nHcC domain of the NTNHA molecule moves like a wing along the axis connecting nHcN and nHcC (see supplementary video 3). Movement of the nHcC wing and the "Most-spread form" of the NTNHA (center) are based on the solution structure of NTNHA. The combined motions of the nHcC wing would be captured as a spread solution structure (right). Elongated "tail"-like structure (indicated with dotted lines) observed in the solution structure might be due to flexibility of the nHcC domain in solution. (For interpretation of the references to color in this figure legend, the reader is referred to the web version of this article.)

lateral orientation. The flexibility of the HcC domain in BoNT was also noted previously [22]. Gu et al. [7] demonstrated that serotype A BoNT in M-TC form (BoNT/NTNHA) displayed a distinct conformation, in contrast to the BoNT in free form, in which the HcC domain rotated about 140 ° around the linker connecting HcN and HcC. Dynamics of the nHcC domain in NTNHA and the HcC domain in BoNT may contribute to form the M-TC. Single-molecule analysis will be needed to fully understand the dynamics of the NTNHA molecule.

Acknowledgment

This research was supported by KAKENHI provided by MEXT/JSPS (for T.W., Grant No. 22590405).

Appendix A. Supplementary data

Supplementary data associated with this article can be found, in the online version, at http://dx.doi.org/10.1016/j.bbrc.2012.07.077.

References

[1] K. Miyata, T. Yoneyama, T. Suzuki, H. Kouguchi, K. Inui, K. Niwa, T. Watanabe, T. Ohyama, Expression and stability of the nontoxic component of the botulinum toxin complex, Biochem. Biophys. Res. Commun. 384 (2009) 126–130.

[2] K. Niwa, K. Koyama, S. Inoue, T. Suzuki, K. Hasegawa, T. Watanabe, T. Ikeda, T. Ohyama, Role of nontoxic components of serotype D botulinum toxin complex in permeation through a Caco-2 cell monolayer, a model for intestinal epithelium, FEMS Immunol. Med. Microbiol. 49 (2007) 346–352.

[3] T. Yoneyama, K. Miyata, T. Chikai, A. Mikami, T. Suzuki, K. Hasegawa, T. Ikeda, T. Watanabe, T. Ohyama, K. Niwa, *Clostridium botulinum* serotype D neurotoxin and toxin complex bind to bovine aortic endothelial cells via sialic acid, FEMS Immunol. Med. Microbiol. 54 (2008) 290–298.

[4] K. Hasegawa, T. Watanabe, T. Suzuki, A. Yamano, T. Oikawa, Y. Sato, H. Kouguchi, T. Yoneyama, K. Niwa, T. Ikeda, T. Ohyama, A novel subunit structure of *Clostridium botulinum* serotype D toxin complex with three extended arms, J. Biol. Chem. 282 (2007) 24777–24783.

[5] H. Kouguchi, T. Watanabe, Y. Sagane, H. Sunagawa, T. Ohyama, *In vitro* reconstitution of the *Clostridium botulinum* type D progenitor toxin, J. Biol. Chem. 277 (2002) 2650–2656.

[6] S. Mutoh, H. Kouguchi, Y. Sagane, T. Suzuki, K. Hasegawa, T. Watanabe, T. Ohyama, Complete subunit structure of the *Clostridium botulinum* type D toxin complex via intermediate assembly with nontoxic components, Biochemistry 42 (2003) 10991–10997.

[7] S. Gu, S. Rumpel, J. Zhou, J. Strotmeier, H. Bigalke, K. Perry, C.B. Shoemaker, A. Rummel, R. Jin, Botulinum neurotoxin is shielded by NTNHA in an interlocked complex, Science 335 (2012) 977–981.

[8] K. Hasegawa, T. Watanabe, H. Sato, Y. Sagane, S. Mutoh, T. Suzuki, A. Yamano, H. Kouguchi, K. Takeshi, A. Kamaguchi, Y. Fujinaga, K. Oguma, T. Ohyama, Characterization of toxin complex produced by a unique strain of *Clostridium botulinum* serotype D 4947, Protein J. 23 (2004) 371–378.

[9] Y. Sagane, T. Watanabe, H. Kouguchi, H. Sunagawa, S. Obata, K. Oguma, T. Ohyama, Spontaneous nicking in the nontoxic-nonhemagglutinin component of the *Clostridium botulinum* toxin complex, Biochem. Biophys. Res. Commun. 292 (2002) 434–440.

[10] K. Miyata, K. Inui, S.-I. Miyashita, Y. Sagane, K. Hasegawa, T. Matsumoto, A. Yamano, K. Niwa, T. Watanabe, T. Ohyama, Crystallization and preliminary X-ray analysis of the *Clostridium botulinum* type D nontoxic nonhaemagglutinin, Acta Crystallogr. F68 (2012) 227–230.

[11] Collaborative Computational Project, Number 4, The CCP4 suite: programs for protein crystallography, Acta Crystallogr. D50 (1994) 760–763.

[12] A. Vagin, A. Teplyakov, MOLREP: an automated program for molecular replacement, J. Appl. Crystallogr. 30 (1997) 1022–1025.

[13] P. Emsley, K. Cowtan, Coot: model-building tools for molecular graphics, Acta Crystallogr. D60 (2004) 2126–2132.

[14] G.N. Murshudov, A.A. Vagin, E.J. Dodson, Refinement of macromolecular structures by the maximum-likelihood method, Acta Crystallogr. D53 (1997) 240–255.

[15] L. Potterton, S. McNicholas, E. Krissinel, J. Gruber, K. Cowtan, P. Emsley, G.N. Murshudov, S. Cohen, A. Perrakis, M. Noble, Developments in the CCP4 molecular-graphics project, Acta Crystallogr. D60 (2004) 2288–2294.

[16] P.V. Konarev, V.V. Volkov, A.V. Sokolova, M.H.J. Koch, D.I. Svergun, *PRIMUS*: a Windows PC-based system for small-angle scattering data analysis, J. Appl. Crystallogr. 36 (2003) 1277–1282.

[17] M.V. Petoukhov, P.V. Konarev, A.G. Kikhney, D.I. Svergun, *ATSAS* 2.1 - towards automated and web-supported small-angle scattering data analysis, J. Appl. Crystallogr. 40 (2007) s223–s228.

[18] K. Inui, Y. Sagane, K. Miyata, S.-I. Miyashita, T. Suzuki, Y. Shikamori, T. Ohyama, K. Niwa, T. Watanabe, Toxic and nontoxic components of botulinum neurotoxin complex are evolved from a common ancestral zinc protein, Biochem. Biophys. Res. Commun. 419 (2012) 500–504.

[19] A.G. Murzin, A.M. Lesk, C. Chothia, β-Trefoil fold: Patterns of structure and sequence in the Kunitz inhibitors interleukins-1β and 1α and fibroblast growth factor, J. Mol. Biol. 223 (1992) 531–543.

[20] H. Ito, Y. Sagane, K. Miyata, K. Inui, T. Matsuo, R. Horiuchi, T. Ikeda, T. Suzuki, K. Hasegawa, H. Kouguchi, K. Oguma, K. Niwa, T. Ohyama, T. Watanabe, HA-33 facilitates transport of the serotype D botulinum toxin across a rat intestinal epithelial cell monolayer, FEMS Immunol. Med. Microbiol. 61 (2011) 323–331.

[21] D. Kumaran, S. Eswaramoorthy, W. Furey, J. Navaza, M. Sax, S. Swaminathan, Domain organization in *Clostridium botulinum* neurotoxin type E is unique: its implication in faster translocation, J. Mol. Biol. 386 (2009) 233–245.

[22] G. Schiavo, M. Matteoli, C. Montecucco, Neurotoxins affecting neuroexocytosis, Physiol. Rev. 80 (2000) 717–766.